JOURNAL OF MATERIALS SCIENCE 14 (1979) 125–132

Effect of gas composition on the deposition of ZrC-C mixtures: The bromide process

T. OGAWA, K. IKAWA, K. IWAMOTO
Japan Atomic Energy Research Institute, Tokai-mura, Naka-gun, Ibaraki-ken, Japan

Mixtures of ZrC–C were chemically vapour deposited from gaseous mixtures of zirconium bromides, methane, hydrogen and argon. The effect of gas composition on the deposition behaviour was studied. The experiments have shown that the methane concentration in the feed gas mixture is a crucial factor in determining the deposition rate and the character of the deposit. Chemical equilibria in the Zr–C–H–Br system were calculated and compared with the experimental results.

1. Introduction

In a coated particle fuel for a high temperature gas cooled reactor (HTGR) a spherical kernel of fissile or fertile material is coated with pyrolytic carbon and SiC to act as barriers against release of fission products. ZrC or ZrC–C mixtures with their high melting points and low neutron capture cross-sections are thought capable of replacing SiC which would not endure above 1500° C [1]. However, aspects of the use of ZrC require investigations, among which are the reactions of fission products with and diffusion in the coating, as well as the behaviour under neutron irradiation. In order to prepare pure flat specimens for these investigations, a detailed study on the chemical vapour deposition of ZrC–C is being carried out. The iodide [2], chloride [3] and bromide [4] processes have already been examined. Though the last proved to be most convenient in operation, it failed to produce ZrC without a significant amount of free carbon. The aim of the present study is, therefore, to examine the effect of the initial gas composition on the deposit composition, amount and character using the bromide process. To this end, both experiments and thermodynamic calculations have been carried out.

2. Experimental

2.1. Procedure

The deposition apparatus is drawn schematically in Fig. 1. Argon at 300 cm^3 min^{-1} bubbles through a bromine saturator at 0° C and then flows over zirconium sponge at 600° C. Thus zirconium bromides are continuously generated and fed into the reaction zone. A mixture of hydrogen and methane is supplied independently from the argon which serves to adjust the total flow rate to ~2100 cm^3 min^{-1}. The aperture of the inner tube containing the sponge is at about 700° C, leaving a 10 cm space up to the first substrate. Substrates numbered 1 to 4, front to rear, are positioned at 1280, 1330, 1360 and 1380° C respectively. Fig. 2 shows the substrate, which is composed of a 0.1 mm-thick Mo sheet and a graphite body of

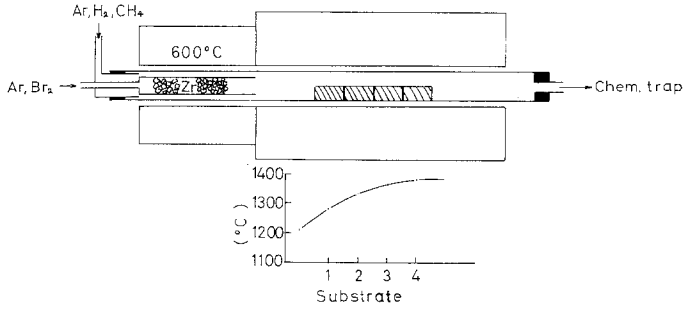

Figure 1 Deposition apparatus.

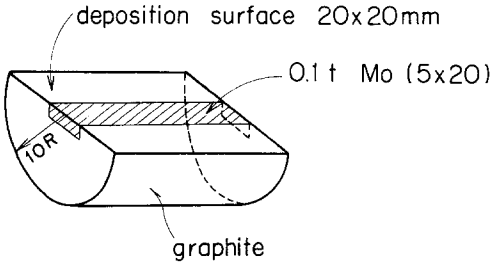

Figure 2 Substrate.

semicircular cross-section, which just fits into the reaction tube.

After deposition of one hour the Mo substrate was separated from the graphite, placed in a Pt boat and burned in an oxygen stream at 1200° C. By weighing ZrO_2 and CO_2, the latter being absorbed in an ascarite tube, the composition of the deposit was obtained. Mo does not interfere with the analysis, since its reaction product with oxygen, MoO_3, sublimes during heating and

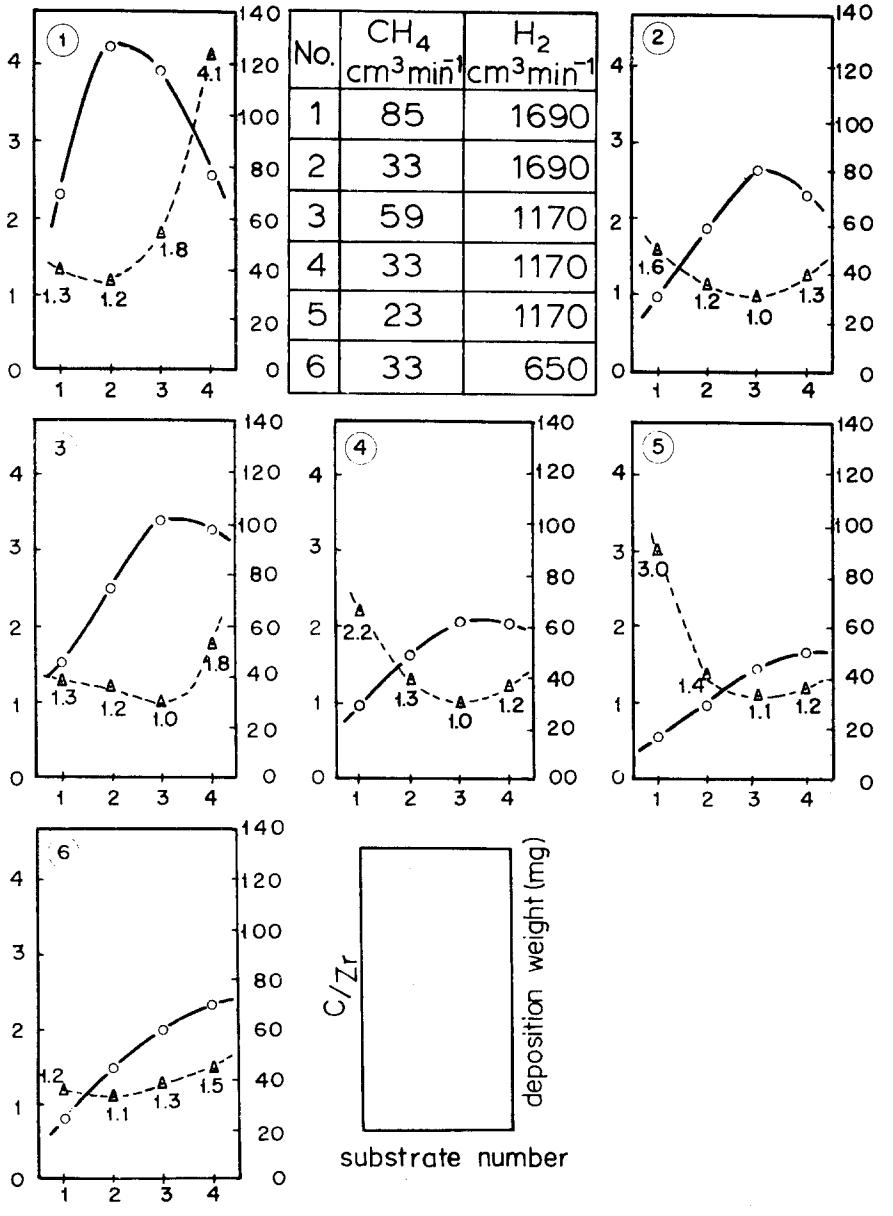

Figure 3 Deposition profiles. Solid line represents deposition weight on 1 cm² Mo substrate; dashed line, deposit composition.

deposits on the colder side of the furnace. Stoichiometric carbide formation was assumed and the amount of the free carbon was taken as the excess of the C/Zr value over 1.0.

The deposit on the graphite substrate was used for characterization using optical microscopic, SEM and X-ray diffraction methods.

2.2. Results

2.2.1. Deposition profile

In Fig. 3 deposition profiles are arranged so that the effect of the gas composition on amount (solid line) and composition (dashed line) of the deposit can be seen. From profiles 6, 4 and 2, one can see the effect of the hydrogen when the methane supply is kept constant; from profiles 5, 4 and 3, the effect of methane when the hydrogen supply is kept constant, and from profiles 6, 3 and 1, the effect of methane or hydrogen when the ratio H_2/CH_4 is kept constant. It is seen that the total deposition amount strongly depends on the methane supply (profiles 5, 4 and 3). Increasing consumption of zirconium over substrates 1 to 3 would be the reason why the peak of the deposition curve becomes pronounced with increase in methane concentration. Hydrogen, however, has a rather trivial influence on the deposition weight within the gas composition range investigated (profiles 6, 4 and 2).

The behaviour of the composition curve is strange. The C/Zr values of substrates 1 and 2 rise with hydrogen increase (profiles 6 and 4), while they decrease with methane increase (profiles 5, and 3). When hydrogen and methane increase simultaneously, keeping the ratio H_2/CH_4 constant, the effects of hydrogen and methane compensate for each other and the C/Zr values for substrates 1 and 2 are relatively constant (profiles 6, 3 and 1). The behaviour seems to contradict the expectation that hydrogen would suppress the methane decomposition and hence its higher partial pressure would results in a lower C/Zr value, and the higher methane partial pressure in a higher C/Zr value.

Figs. 4 and 5 are derived from Fig. 3. The sums of the amounts of zirconium, total carbon and free carbon for substrates 1, 2 and 3 are shown. The deposition weights for substrate 4 are omitted because the supersaturation of zirconium bromides is thought to have decreased significantly, as already stated. Fig. 4 shows that hydrogen does not greatly suppress or affect the overall free carbon formation. Though total carbon increases

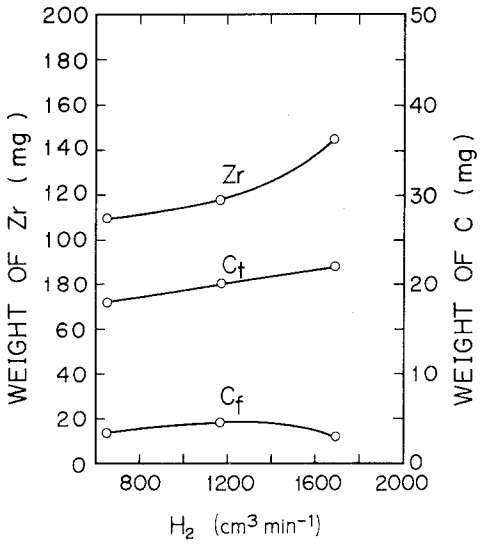

Figure 4 Effect of hydrogen supply on the deposition of Zr, free carbon (C_f) and total carbon (C_t).

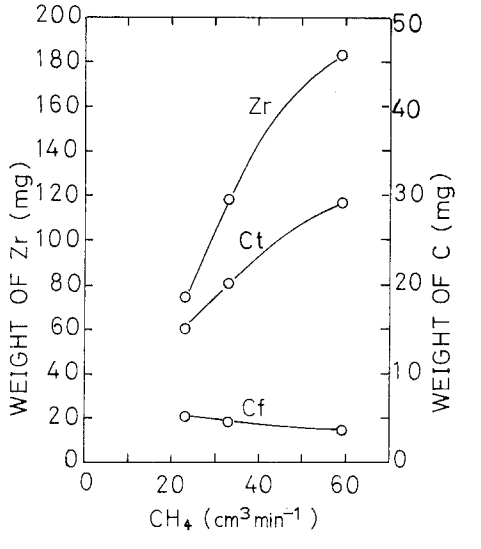

Figure 5 Effect of methane supply on the deposition amount of Zr, free carbon (C_f) and total carbon (C_t).

with increase of hydrogen flow, it is due to zirconium deposition as carbide. Thus the influence of hydrogen is not necessarily inconsistent with the expectations mentioned above. The influence of methane, however, is inconsistent with the expectation. Fig. 5 shows that, with increase in methane availability, the amount of ZrC increases, but that of free carbon decreases.

2.2.2. Characterization

Fig. 6 summarizes the relation between the surface morphology and the deposition condition. Circled

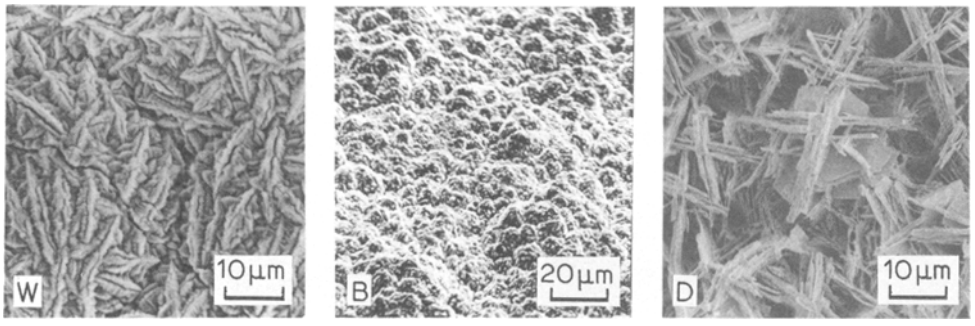

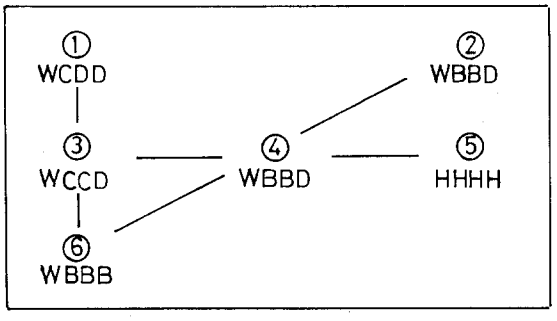

Figure 6 Surface morphology and gas composition. Circled numbers denote the runs as shown in Fig. 3 and capital letters the morphologies: (W) wrinkled, (B) blistered, (D) dendritic, (C) crystalline, (H) horn-like.

numbers denote the runs (see Fig. 3) and capital letters the morphologies as shown in Fig. 6. The letters from left to right indicate the morphology of the substrates 1 to 4.

It can be seen that methane plays a significant part in determining the morphology. In run 5 the methane supply is not enough to produce a coherent coating (Fig. 6H). When the amount of methane increased in run 4 a coating with a blister appearance (Fig. 6B) resulted. When the amount of methane was increased further in run 3, a crystalline coating (Fig. 6C) with columnar microstructure (Fig. 7) resulted. On the other hand the variation of hydrogen flow has little influence

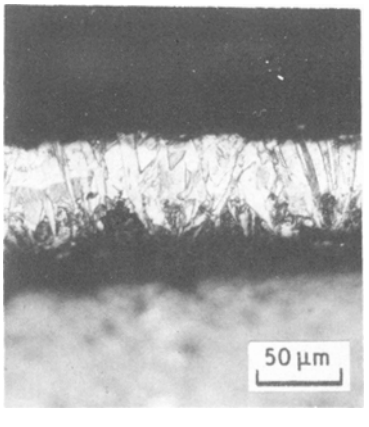

Figure 7 Microstructure of the crystalline coating (Fig. 6C).

on the forms of the coatings (profiles 6, 4 and 2). The fact that the morphology is also dependent on the substrate position is considered to be attributable to two factors, namely, the temperature at which the reaction takes place, and the zirconium bromide supersaturation level over each substrate. In run 3, for instance, for substrate 1 the presence of enough bromide and a low temperature produced a wrinkled or rather featureless coating (Fig. 6W); for substrates 2 and 3 the bromide concentration and a high temperature gave a crystalline coating (Fig. 6C); and for substrate 4 a low supersaturation of bromides in consequence of consumption by substrates 1 to 3 resulted in a dendritic appearance (Fig. 6D). It should be noted that in run 3 the methane supply is sufficient, but when it is insufficient as in run 5, even a combination of a high supersaturation of zirconium bromides and a high temperature does not produce coherent coatings.

The crystallographic orientation was studied by X-ray diffraction. The intensity ratio $I(2\,2\,0)/I(1\,1\,1)$ of ZrC on substrate 3 is shown in Fig. 8. The dashed line represents the intensity ratio of powdered ZrC as a reference. Here again the dependence on initial gas composition is evident. With increase in the amount of methane, ZrC crystals tend to orient themselves with {1 1 0} planes parallel to the deposition surface. The same tendency occurs with increase in the amount of hydrogen, but to a lesser extent.

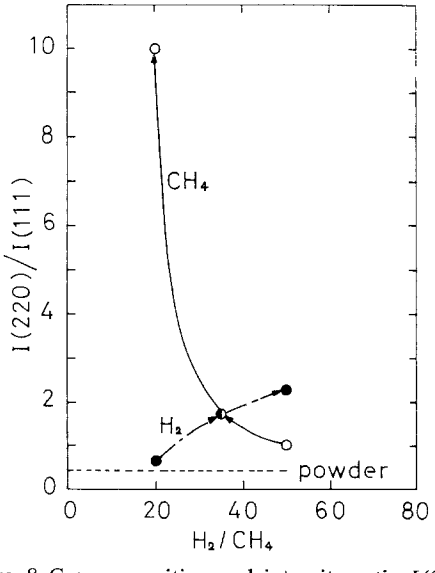

Figure 8 Gas composition and intensity ratio $I(2\,2\,0)/I(1\,1\,1)$ of ZrC. Dashed line indicates the intensity ratio of the powdered ZrC.

3. Calculation of chemical equilibria

3.1. Procedure

The amount and composition of the deposit in chemical equilibrium with the gas phase were computed by applying the free energy minimization method, which was first described by White *et al.* [5], and extended to multiphase equilibria calculation by Eriksson [6–8]. Similar calculations to those presented here have been made by Samoilenko and Pereseleutseva for the Zr–C–H–Cl system, but the formation of ZrC was not considered [9].

In the method a set of variables Y_i which minimizes the quantity

$$(G/RT) = \Sigma Y_i [(g^0/RT)i + \ln a_i]$$

where

G = total free energy of the system,
R = gas constant,
T = thermodynamic temperature,
Y_i = mole number of a substance,
g^0 = standard chemical potential,

and

a_i = activity,

and satisfies the mass balance constraints, is the set for the equilibrium condition. Starting from an arbitrary set of Y_i, an improved set is calculated, which is used as the input for a further calculation. After a series of such iterations, each of which starts with an improved set of Y_i, the equilibrium set is reached. Our program is basically the same as Eriksson's SOLGAS [6], but contains some unique features for application to the Zr–C–H–Br system.

First, the regular solution approximation modified for an interstitial solid solution is applied to the non-stoichiometric ZrC. The NaCl type lattice of ZrC is imagined as separated into a Zr sublattice and a C sublattice, and the latter is regarded as a substitutional solid solution of carbon and its vacancy, following the treatment of Hillert *et al.* on $(Fe, Mn)_3C$ [10]. Hence the molar free energy of the C sublattice can be written formally as follows:

$$G_{CV}^{ZrC} = Y_C^0 G_C^{ZrC} + Y_V^0 G_V^{ZrC} + RT(Y_C \ln Y_C + Y_V \ln Y_V) + Y_C Y_V \Omega$$

where

${}^0G_C^{ZrC}$ = molar free energy of C sublattice without vacancies,

$^0G_V^{ZrC}$ = molar free energy of the vacancy making the same lattice as the C sublattice,

Y_C = molar fraction of carbon,

Y_V = molar fraction of the vacancy,

and

Ω = interaction parameter.

If we note that

$$Y_C + Y_V = 1$$

and

$$^0G_{Zr}^{ZrC} + {}^0G_C^{ZrC} = {}^0G_{ZrC}$$
$$^0G_{Zr}^{ZrC} + {}^0G_V^{ZrC} = {}^0G_{Zr}$$

where

$^0G_{Zr}^{ZrC}$ = molar free energy of Zr sublattice,

$^0G_{ZrC}$ = molar free energy of stoichiometric ZrC,

and

$^0G_{Zr}$ = molar free energy of Zr,

then we can write the equation for the molar free energy of the non-stoichiometric ZrC as follows:

$$\begin{aligned} G_{ZrCx} &= G_{Zr}^{ZrC} + G_{CV}^{ZrC} \\ &= Y_C {}^0G_{ZrC} + Y_V {}^0G_{Zr} \\ &\quad + RT(Y_C \ln Y_C + Y_V \ln Y_V) \\ &\quad + Y_C Y_V \Omega. \end{aligned}$$

From this equation the composition dependence of the zirconium activity is derived. The interaction parameter Ω was chosen so as to give the best fit to the reported activity in non-stoichiometric ZrC. For this purpose the linear dependence of Ω on Y_V was assumed [11]. Though the zirconium activity in ZrC has been measured as a function of composition and temperature between 1700 and 2200 K by Storms and Griffin, the values reported are only valid above 2125 K [12]. We have extrapolated those values to the lower temperatures; at 1800 K, for instance, $\Omega = -28600 + 44600\, Y_V$ (cal mol^{-1}) was derived. Such a tentative value suffices to estimate qualitatively the effect of the initial gas composition.

Another feature concerns the selection of the solid system. Possible solid systems are (a) Zr + $ZrC_{0.55}$, (b) non-stoichiometric ZrC and (c) ZrC + C. The iteration to calculate the equilibrium composition starts from system (a), and then proceeds selecting one system out of the three according to the composition at each iteration step. When the amount of Zr in (a), or C in (c), becomes virtually zero during the iteration, the system is altered to (b), and when C/Zr goes beyond the boundaries of the ZrC phase, the system is altered from (b) to (a) or (c). The lower and the upper boundaries of the ZrC phase where set at C/Zr = 0.55 and 0.999 respectively [12, 13].

The gaseous species considered were $ZrBr_4$, $ZrBr_3$, $ZrBr_2$, Br_2, Br, HBr, CH_4, CH_3, C_2H_2, H_2 and H. All thermodynamic data except that of the non-stoichiometric ZrC were found in the JANAF tables [14]. Similar input gas compositions Zr : C : H : Br were chosen for the experimental gas compositions. Zr/Br = 0.25 was assumed, implying that $ZrBr_4$ would be the main bromide to flow into the reaction zone. The value is possibly overestimated, because the conversion of bromine to the bromide would not be complete and lower bromides ($ZrBr_3$, $ZrBr_2$) with low vapour pressures [15, 16] might also be formed. A total pressure of 1 atm. was assumed throughout all the calculations.

3.2. Results of calculation

Fig. 9 shows the estimated effect of hydrogen supply. Hydrogen suppresses free carbon formation, but increases ZrC deposition, though the ultimate ZrC formation is determined by methane supply. Above a certain point (~20 mol % H) the effect of hydrogen becomes very small, except that the C/Zr value goes on decreasing slightly. The description agrees qualitatively with the experimental results (Figs. 3 and 4).

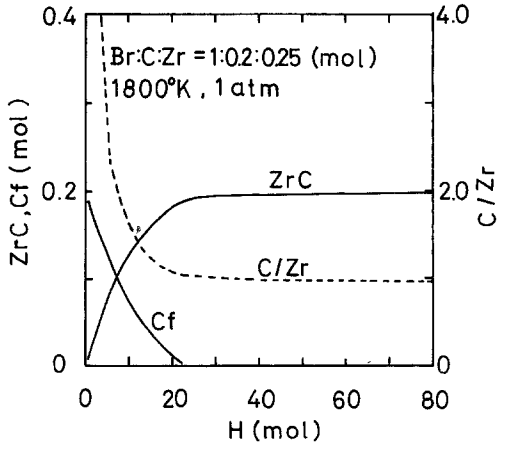

Figure 9 Result of calculation: effect of hydrogen supply.

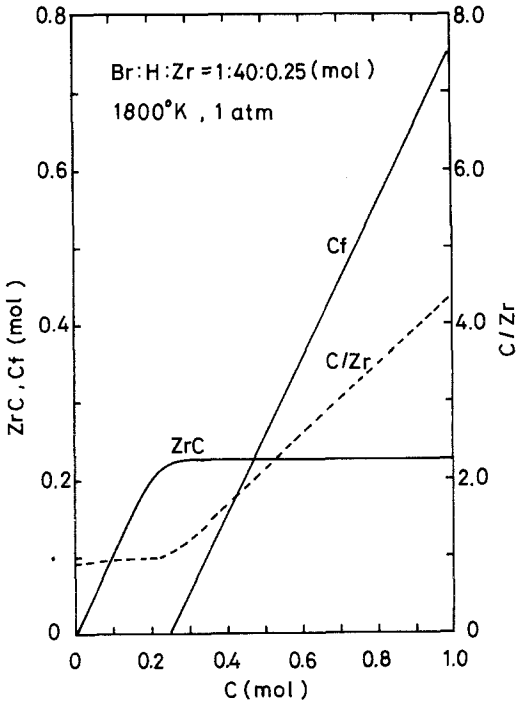

Figure 10 Result of calculation: effect of methane supply.

Fig. 10 is a description of the estimated effect of methane supply. There is a range (~0.25 mol% C) over which the methane supply has an appreciable effect on the extent of deposition, but little effect on the deposit composition. Above that range the free carbon formation becomes significant with increase in the amount of methane. Here the thermodynamic prediction differs a little from the experimental results, because the increasing methane supply suppresses free carbon formation in the experiment (Fig. 5).

4. Discussion

In a thermodynamic description of SiC deposition from the mixture of $SiCl_4$ and CH_4, Si deposition is stated to be independent of C deposition [17]. This is not the case in the chemical vapour deposition of ZrC. It is shown by both calculation and experiment that Zr deposition and C deposition are much interrelated. However, there is a difference between the results of calculation and those of experiment. The thermodynamic calculation predicts that the free carbon formation rises with methane, but experiment showed the converse within the investigated gas composition range. In order to explain the tendency of free carbon formation, morphology and preferred orientation with methane concentration change, a model is proposed on the basis of an existing model of pyrolytic carbon deposition.

Grisdale [18] elucidated carbon deposition by the droplet mechanism as follows. During pyrolysis of a gaseous hydrocarbon a suspension of liquid or plastic droplets of complex organic materials is formed and the droplets impinge on the surface in a reaction chamber. When deposited at a relatively low rate, the droplets are dehydrogenated to carbon keeping their spherical shape. Therefore the resulting surface exhibits a spherical shape of roughness and a poor degree of preferred orientation. On the other hand the number of droplets available per unit time increases with hydrocarbon concentration, and the average viscosity decreases since the average duration between their formation and impingement on the surface decreases. Hence the droplets are deformed and smeared over the surface. The deposit thus has a relatively smooth surface and a large degree of preferred orientation.

Now if it is assumed that ZrC is formed by the reaction of zirconium or zirconium bromides with these organic droplets, the variation of morphology and preferred orientation is explained along the lines of the argument above. Also, the tendency of the less free carbon formation with the larger methane concentration is also explained. As methane concentration increases the droplets change their shape from spherical to smeared, resulting in an increase of the surface area which comes into contact with zirconium or zirconium bromides. Thus the reaction to form ZrC becomes more vigorous and free carbon formation is suppressed.

Because there is no direct evidence as yet to support the present model, too much emphasis should not be placed on it. If the form of free carbon in the deposit can be made clear in the future, this evidence will test the model.

5. Conclusion

Experiments and thermodynamic analyses on the effect of gas composition on the chemical vapour deposition of ZrC–C have been made. Experimental results confirmed the following:

(1) Hydrogen has little effect on the amount and character of the deposit within the gas composition range investigated.

(2) The extent of deposition is dependent on the methane supply. When the methane supply is insufficient, the deposit does not form a coherent

coating. With a sufficient methane supply the deposit becomes a crystalline coherent coating and ZrC crystals tend to orient themselves with {1 1 0} planes parallel to the deposition surface.

The overall behaviour of deposition was similar to the results of the thermodynamic calculation, except that within a certain gas composition range increasing methane supply suppressed free carbon formation. In order to explain this discrepancy a model based on the droplet mechanism of pyrolytic carbon deposition has been proposed.

Acknowledgements

We wish to thank, Dr S. Nomura and Dr J. Shimokawa, Head and Deputy Head of Nuclear Fuel Research Division, JAERI, for their interest and encouragement, and our colleagues K. Kobayashi and K. Fukuda for their helpful advice.

References

1. K. FUKUDA and K. IWAMOTO, JAERI-M 6311 (1975).
2. K. IKAWA, *J. Less-Common Metals* **27** (1972) 325.
3. *Idem, ibid.* **29** (1972) 233.
4. *Idem, ibid.* **44** (1976) 207.
5. W. B. WHITE, S. M. JOHNSON and G. B. DANTZIG, *J. Chem. Phys.* **28** (1958) 751.
6. G. ERIKSSON, *Acta Chem. Scand.* **25** (1971) 2651.
7. G. ERIKSSON and E. ROSEN, *Chem. Scripta* **4** (1973) 193.
8. G. ERIKSSON, *ibid.* **8** (1975) 100.
9. V. G. SAMOILENKO and L. N. PERESELEUTSEVA, *Poroshkovaya Metallurgiya* **153** (1975) 35.
10. M. HILLERT, T. WADA and H. WADA, *J. Iron Steel Inst.* **189** (1967) 539.
11. T. NISHIZAWA, *Nippon Kinzokugakkai Kaiho* **12** (1973) 189.
12. E. K. STORMS and J. GRIFFIN, *High Temp. Sci.* **5** (1973) 291.
13. E. K. STORMS, editor, "The Refractory Carbide" (Academic Press, New York, 1967) p.18.
14. D. R. STULL, editor, "JANAF Thermochemical Tables", Gull Clearing House Document PB 168 370.
15. "Gmelins Handbuch der Anorganischen Chemie", Vol. 8, No. 42 (Verlag Chemie, Weinheim, 1958) p. 314.
16. H. L. SCHLÄFER and H. SKOLUDEK, *Z. anorg. allg. Chem.* **316** (1962) 15.
17. J. E. DOHERTY, *J. Met.* **28** (1976) 6.
18. R. O. GRISDALE, *J. Appl. Phys.* **24** (1963) 1082.

Received 8 August 1977 and accepted 15 May 1978.